SOILS AND FOUNDATIONS Vol. 19, No. 2, June 1979
Japanese Society of Soil Mechanics and Foundation Engineering

THE INFLUENCE OF STRESS HISTORY AND STRESS SYSTEM ON THE STRESS-STRAIN-STRENGTH PROPERTIES OF SATURATED CLAY

Toshiyuki Mitachi* and Shigeru Kitago**

ABSTRACT

Undrained triaxial compression and extension stress-strain behaviour of a saturated remolded clay consolidated under K_0 and isotropic stress conditions was investigated. Test results indicate that octahedral stress ratio-strain relationship and effective stress path in octahedral stress space were affected by the stress system during shear as well as the stress condition during consolidation. Moreover, it was also found that not only undrained shear strength but also effective angle of shearing resistance were influenced by the two factors mentioned above. Octahedral stress ratio versus dilatancy curve was approximately represented by a set of two straight lines.

Based on the test results, the authors proposed a new method of predicting undrained stress-strain behaviour of K_0 consolidated clay by using the data obtained from isotropically consolidated undrained tests.

Key words: angle of internal friction, anisotropy, clay, consolidated undrained shear, dilatancy, effective stress, shear strength, stress path, stress-strain curve, triaxial compression test

IGC: D 6/D 5

INTRODUCTION

Geotechnical problems in practice such as slope stability or bearing capacity of foundation are usually solved by using the strength parameters obtained from triaxial compression test conducted under initial isotropic stress condition. However, the stress and strain conditions of soil elements differ from each other by the position they exist in situ. In general, the stress-strain-strength properties of soils are greatly influenced by the stress or strain to which they have been or will be subjected before or during shear. Although it is desirable to test soils under exactly the same conditions as those in situ, laboratory strength tests are usually performed under the condition of isotropically consolidated triaxial compression. Therefore, from the practical point of view, real stress-strain-strength properties of soils which might be obtained only by the special tests simulating the stress and strain conditions in situ would be conveniently related to those obtained from conventional tests for design purpose.

In this paper, the influence of stress condition during consolidation and stress system during shear on the undrained stress-strain-strength properties of a saturated remolded clay are presented. A new method to predict the stress-strain behaviour of K_0 consoli-

* Associate Professor, Department of Civil Engineering, Hokkaido University, Sapporo, Hokkaido.
** Professor, Department of Civil Engineering, Hokkaido University, Sapporo, Hokkaido.
Written discussions on this paper should be submitted before April 1, 1980.

dated clay using the parameters obtained from conventional triaxial tests is also presented.

EXPERIMENTS

Clay Tested

A remolded clay, LL and PI of which are 86% and 49% respectively, was sampled at a site of river improvement near Sapporo, and was thoroughly mixed with distilled water, sieved by a 420μ size sieve and stored in the state of slurry. Before making test specimen, the slurry was stirred again in a soil mixer for about an hour and then transfered under a vacuum into a preconsolidation cell, 350mm high and 165mm in diameter. Then the slurry was initially consolidated one-dimentionally under an axial stress of 78kPa for about 4 days. Specimens, 120mm high and 50mm in diameter, trimmed from this preconsolidated sample were then further consolidated isotropically or anisotropically in the triaxial cell and then sheared under undrained condition.

Testing Procedure

Six series of consolidated undrained triaxial test were performed under following conditions.

(1) *NIC* Test; Specimens are consolidated isotropically and then sheared under undrained compression by increasing axial stress while lateral stress is maintained constant.

(2) *NIE* Test; After isotropic consolidation, specimens are sheared under undrained extension by decreasing axial stress while lateral stress is maintained constant.

(3) *NIEL* Test; Same as *NIE* test but with axial stress constant and lateral stress increased.

(4) NK_0C Test; Before undrained compression, specimens are consolidated under K_0 condition.

(5) NK_0E Test; After K_0 consolidation, specimens are sheared by decreasing axial stress while lateral stress is maintained constant.

(6) NK_0EL Test; Same as NK_0E test but with axial stress constant and lateral stress increased.

NIC and *NIE* tests were carried out with conventional triaxial apparatus. During the consolidation process of NK_0C and NK_0E tests, automatic K_0 control system (Mitachi and Kitago, 1976) was connected to the conventional triaxial apparatus just prior to K_0 consolidation, and for the shear stage of *NIEL* and NK_0EL test, the apparatus shown schematically in Fig. 1 was used to perform strain controlled test by increasing lateral stress. The loading ram of the triaxial cell is sealed to the head of the top cap by means of Bellofram. The control cylinder connected to the cell is filled with water which is pushed at a constant rate into the cell to increase all-round pressure.

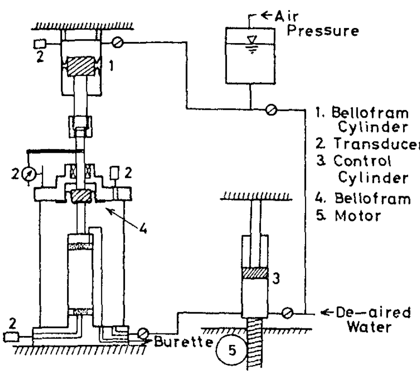

Fig. 1. Schematic diagram of loading extension test apparatus

Since variation of both cell pressure and sectional area of the specimen in *NIEL* and NK_0EL tests changes the value of axial stress, air pressure in the upper room of the Bellofram cylinder was manually controlled to cancel the axial stress change in order to maintain the axial stress constant.

During the consolidation stage of all the tests involved, all-round pressure was increased in several steps, and so the consolidation took 3 to 6 days in isotropic condition and 6 to 9 days in K_0 condition depending on the magnitude of the final pressure. Consolidation duration after reaching the final cell pressure was specified to be 24 hours in both K_0 and

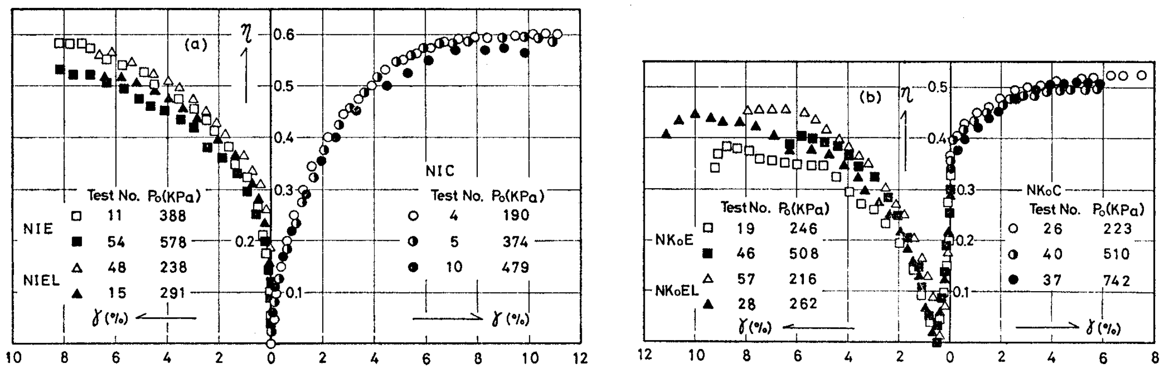

Fig. 2. Octahedral stress ratio vs. strain relationship

isotropic conditions. Initial back pressure of 98kPa was applied to all specimens. The rate of axial strain in undrained shear was 0.04%/min. for all tests and pore pressure was measured at the bottom of the specimen.

TEST RESULTS AND DISCUSSION

Stress Ratio-Strain Relationship and Effective Stress Path

Fig. 2(a) and (b) illustrate the octahedral stress ratio-strain relationship for 6 series of test. In these figures, η represents the ratio of octahedral shear stress τ to octahedral effective normal stress p, and γ and p_0 are octahedral shear strain and octahedral effective normal stress after consolidation, respectively. As can be seen from these figures, the stress ratio-strain curves in each test series are almost the same irrespective of the magnitude of consolidation pressure, and the curves of *NIEL* test almost coincide with those of *NIE* test. This may also be true for the relationship between NK_0EL and NK_0E test, although the scattering of the data is relatively large.

In *NIE* and *NIEL* test, axial stress is equal to the minor principal stress σ_3', and the other two principal stresses σ_1', σ_2' are equal to each other in magnitude and major one, whereas in *NIC* test σ_2' is equal to σ_3'. In NK_0E and NK_0EL test, however, axial stress remains initially as major principal stress until the interchange in principal stress directions takes place at about 0.5% of octahedral shear strain, and thereafter it is transfered to minor one. On the other hand, in NK_0C test, axial stress is always the major principal stress, because the interchange in principal stress directions does not occur in this test, and the cell pressure is always the minor principal stress, which is equal to the intermediate one in magnitude. Therefore, it can be concluded that the difference of stress system (or the difference of relative magnitude of intermediate stress) during shear affects the stress ratio-strain relationship, but the type of stress application, i. e. increasing

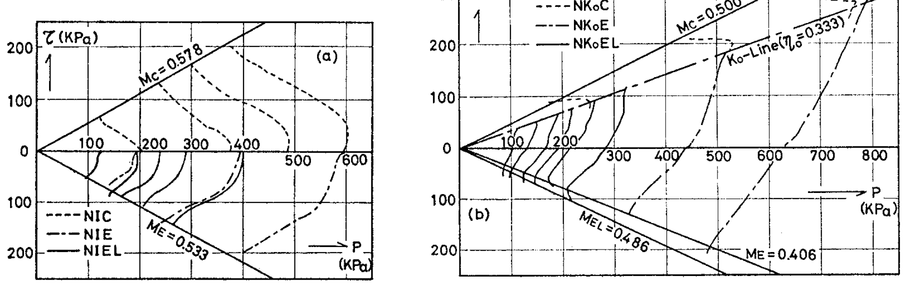

Fig. 3. Effective stress paths in octahedral stress space

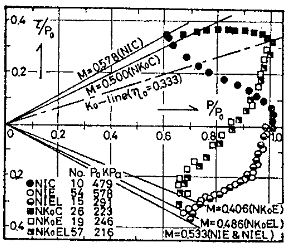

Fig. 4. Comparison of normalized stress paths obtained from six series of test

or decreasing stress, in extension tests gives little influence upon the stress ratio–strain properties of clay, irrespective of the stress system during consolidation.

Fig. 3 (a) and (b) show the effective stress paths in the octahedral stress space for 6 series of test. Fig. 4 illustrates typical stress paths among the 6 series of test, normalized by the octahedral effective normal stress after consolidation. Parry and Nadarajah (1973) reported that there is a distinct measure of symmetry about the $\tau=0$ line for compression and extension test stress paths for isotropically consolidated specimens. As can be seen in Fig. 3 or 4, however, the test results of the present authors do not show the symmetry of stress paths.

The stress paths for both *NIE* and *NIEL* test in Fig. 4 seem to almost coincide with each other. This coincidence is also seen between the stress paths of NK_0E and NK_0EL test.

From the η vs. γ and τ vs. p relationships mentioned above, it may be concluded that the type of stress application, i. e. increasing or decreasing stress, during shear does not affect the effective stress–strain behaviour of clay irrespective of the stress system during consolidation, as far as the magnitude of σ_2' during shear is equal to σ_1' or it is equal to σ_3'.

Effective Strength Parameter ϕ', and Undrained Shear Strength

Effective angle of shearing resistance ϕ' determined from the deviator stress maximum criterion, and the ratio of undrained shear strength s_u to effective vertical consolidation pressure p_v for 6 series of test are listed in Table 1. Paying attention to the ϕ' values

Table 1. Strength parameters obtained from the present six series of test including those from earlier ones (Kitago et al., 1976)

Consol. Condition	ϕ_C' (°)	ϕ_E' (°)	ϕ_{EL}' (°)	$\sin\phi_C'/\sin\phi_E'$	$(s_u/p_v)_C$	$(s_u/p_v)_E$	$(s_u/p_v)_{EL}$	$(s_u/p_v)_C/(s_u/p_v)_E$	PI(%)
Iso.	30.6	44.2	44.4	0.73	0.383	0.382	0.405	0.95	49
K_0	26.8	30.2	38.5	0.90	0.301	0.192	0.235	1.57	49
Iso. ('76)	34.5	46.1	—	0.79	0.40	0.38	—	1.05	20
K_0 ('76)	32.0	42.4	—	0.79	0.32	0.21	—	1.52	20

Table 2. Comparison of published data on strength parameters obtained from undrained compression and extension tests

Authors	Henkel ('60)	Parry ('60)	Parry et al. ('73)		Ladd ('65)	Vaid et al. ('74)	Leon et al. ('77)	Lade ('76)	Shibata et al. ('65)	Wu et al. ('63)	Broms et al. ('65)
Consol. Condition	Iso.	Iso.	Iso.	K_0	K_0	K_0	Iso.	Iso.	Iso.	Iso.	Iso.
ϕ_C' (°)	21.7	22.6	22.6	20.8	26.5	29.8	44	29.3	33.7	33.2	29.2
ϕ_E' (°)	21.1	21.3	20.5	28.0	38.8	33.8	78	32.5	33.7	33.1	36.0
$\sin\phi_C'/\sin\phi_E'$	1.03	1.06	1.10	0.75	0.71	0.89	0.71	0.91	1.00	1.00	0.83
$(s_u/p_v)_C$	0.28	0.29	0.215	0.205	0.33	0.268	0.51	0.49	0.42	0.50	0.43
$(s_u/p_v)_E$	0.23	0.24	0.205	0.175	0.165	0.168	0.51	0.45	0.37	0.33	0.34
$(s_u/p_v)_C/(s_u/p_v)_E$	1.22	1.21	1.05	1.17	2.00	1.59	1.00	1.09	1.14	1.52	1.26
PI (%)	25	25	32	32	15	18	290	30	49	24	25

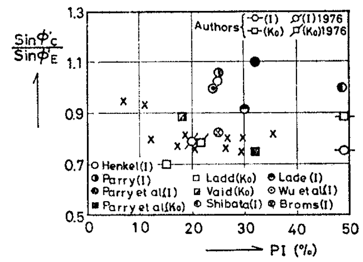

Fig. 5. Ratio of ϕ' value by compression to that by extension tests

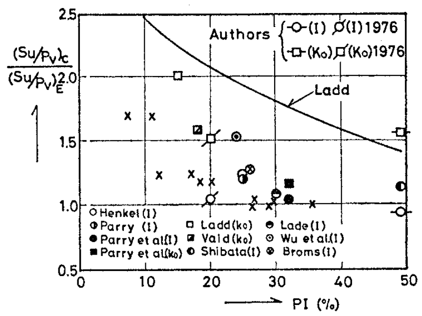

Fig. 6. Undrained strength ratio vs. plasticity index

of extension tests, those of NIE and $NIEL$ are almost coincident, but those of NK_0E and NK_0EL differ as much as 8 degrees. This difference can be attributed to significant development of pore pressure in NK_0EL test, reducing the effective mean stress at failure as small as 200kPa, whereas the cell pressure at failure rose as high as 800kPa. Thus the data points at failure concentrated around the range of 0 to 200kPa of effective mean principal stress as shown in Fig. 3, and this seemed to make the calculated value of ϕ' larger than the actual one.

Table 2 shows the comparison of the published data on ϕ' value, where suffix C and E denote compression and extension test, respectively. Although it has been reported that the stress anisotropy during consolidation does not make any difference on the ϕ' value in compression test for normally consolidated clay (Henkel and Sowa, 1963; Akai and Adachi, 1965; etc.), taking especially into account of the test results by Parry and Nadarajah and those by the present authors, it should rather be concluded that the ϕ' values both in compression and extension are affected to a certain degree by the stress anisotropy during consolidation.

Fig. 5 illustrates the comparison of ϕ' values between compression and extension tests. The values with cross mark in this figure were obtained from the experiments using clay-glass beads mixtures (Kitago et al., 1978) which indicate that the ratio of the ϕ_C' to ϕ_E' decreases with the increase in plasticity index. The test results by other research workers on clay, however, do not exhibit a distinct trend. In any case, the difference between ϕ_C' and ϕ_E' is greater in K_0 consolidated clay than in isotropically consolidated one.

Comparison of published data of undrained shear strength in compression with those in extension is shown in Table 2. Fig. 6 also illustrates the published data on this subject including those of present authors. From this figure and Table 2, it can be seen that the value of s_u/p_v is greatly influenced by the difference of stress system, especially in K_0 consolidated clay. Ladd (1973) performed 3 series of consolidated undrained test and presented the undrained strength ratio of triaxial compression to direct shear, and the ratio of triaxial extension to direct shear. He concluded that each ratio approaches asymptotically to unity as the plasticity index of clay increases. Solid line in Fig. 6 is obtained by using average values of Ladd's data. Cross marks in this figure are the data on clay-glass beads mixtures mentioned above. Although the data points of present authors including those by other research workers have considerable deviation from Ladd's experimental line, they have a general trend that the ratio approaches to unity with the increase of plasticity index.

Recently, Mikasa et al. (1978) reported that the s_u/p_v ratio for K_0 consolidated specimen is almost equal to that for isotropically consolidated one, especially for clays with higher plasticity (PI=75%). This fact and the trend shown in Fig. 6 may probably be subjected to common rule, i. e. the higher the plasticity of clay, the smaller the influences of stress anisotropy during consolidation and stress system during shear on the undrained strength.

Dilatancy Characteristics

Presuming that the total change of void ratio de during shear is represented by the sum of the change due to the increment of effective mean stress $(de)_c$ and that due to the increment of deviatoric stress $(de)_d$, then

$$de=(de)_c+(de)_d \tag{1}$$

and

$$(de)_c=-\lambda dp/p \tag{2}$$

, where λ corresponds to compression index. And if the volumetric strain due to the increment of deviatoric stress is assumed to be a function of octahedral stress ratio η, i. e. $(v)_d=F(\eta)$, then

$$(de)_d=-(1+e_0)F'(\eta)d\eta \tag{3}$$

Combining Eq. (1), (2) and (3) and solving the resultant differential equation with the initial condition $e=e_0$ when $p=p_0$ and $\eta=\eta_0$, the following equation

$$e-e_0=-\lambda \ln p/p_0-(1+e_0)[F(\eta)-F(\eta_0)] \tag{4}$$

can be obtained, where η_0 is the octahedral stress ratio after completion of anisotropic consolidation. For isotropic consolidated undrained shear test, putting the conditions $e=e_0$ and $F(\eta_0)=0$ into Eq. (4), the following equation is obtained.

$$F(\eta)=-\frac{\lambda}{1+e_0}\ln p/p_0 \tag{5}$$

Based on the concept of Scott (1963) on the volume change in the soil structure, Tsushima and Miyakawa (1977) derived a similar equation to Eq. (5) (combining their Eq. (3) with (7), the same form of Eq. (5) of this paper is obtained), and they called the function $F(\eta)$ as equivalent dilatancy. In this paper, it will preferably be called dilatancy function. Ohta et al. (1975) developed a theory for stress-strain relationship for anisotropically consolidated clay, assuming that $F(\eta)=\mu(\eta-\eta_0)$, where μ is a coefficient expressing the dilatancy intensity.

Fig. 7(a) and (b) illustrate the relationship between stress ratio η and dilatancy function $F(\eta)$. In compression test, the observed values for $F(\eta)-\eta$ curves could be approximated by a straight line, excluding their initial parts of positive dilatancy. Hata et al. (1969) infered that the positive dilatancy would disappear if the strain rate is set to be very small. Most research workers interested in the stress-strain behaviour of clays are seen

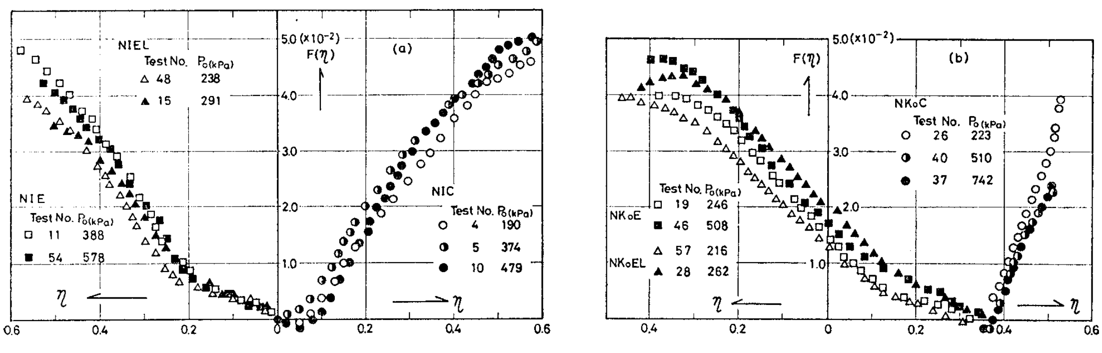

Fig. 7. Octahedral stress ratio vs. dilatancy

to support this inference, but there are some published data which do not support this (e.g. Sawada et al., 1977). Moreover, Shibata et al. (1976) mentioned that even though the strain rate is set to be extremely small, the deviation of the observed $F(\eta)-\eta$ relationship from Ohta's assumption will be large with the increase of silt and sand fraction of a given soil. Therefore, the present authors presume that positive dilatancy develops in the initial part of shear within the conventional strain rate range used in the undrained test. In later part of this paper, a new method of estimating the stress-strain behaviour of K_0 consolidated clay will be proposed by using the $F(\eta)-\eta$ relationship obtained from isotropically consolidated undrained tests.

Comparison of Observed and Predicted Stress-Strain Behaviour by Existing Theories

The authors intended to find out a method to predict the stress-strain relationship of K_0 consolidated clay, using the parameters obtained from the conventional consolidated undrained (CU) triaxial test results. To do this, they began with establishing an appropriate stress-strain theory for predicting the isotropically consolidated undrained case, and then, in order to apply this theory to the K_0 consolidated clay, they made some modifications to the theory so as to fill up the discrepancy which comes from the stress and the structural anisotropy resulting from K_0 consolidation.

Now, the validity of the existing theories is examined, using the present CU triaxial test results. The test data used for this purpose are from *NIC*-No. 4 and the computed parameters are as follows.

$M=0.578 \quad \lambda=0.221 \quad \kappa=0.113 \quad e_0=1.339$

, where M is equal to η at critical state, λ and κ correspond to compression and swelling indices, respectively and e_0 is void ratio after consolidation. M and λ are average values obtained from the series of *NIC* tests. Determination of the value of κ is not easy in general because of the non-linearity of swelling line. Following the suggestion by Karube (1975), its value was obtained by drawing a line passing observed two points which locate far away from the virgin consolidation line.

Fig. 8 (a) shows the comparison of observed stress path and stress ratio-strain relationship with calculated ones by original Cam-Clay equation (Roscoe et al., 1963). In this figure, calculated stress paths and stress ratio-strain relationships for additional two cases assuming $\kappa/\lambda=0.3$ and $\kappa/\lambda=0.1$ with the fixed value of $\lambda=0.221$ are also illustrated. Calculated stress ratio versus strain curve for $\kappa/\lambda=0.5$ follows approximately the observed values. On the other hand, effective mean stress p in the predicted stress paths monotonously decreases as shear

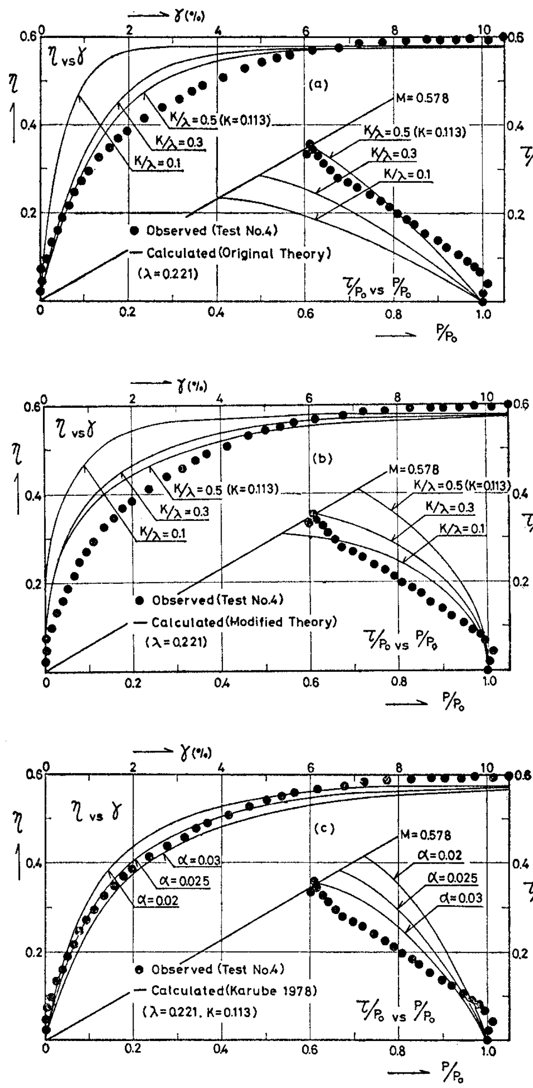

Fig. 8. Observed and predicted stress-strain relationship by existing theories

stress increases toward the critical state point, whereas in the measured stress path p increases slightly in the earlier part of shear. Thus, the stress paths predicted by the original theory show an appreciable difference from the observed ones, and this can be demonstrated by the data from other tests of the present study.

It should be noted that the pattern of predicted stress path and stress ratio-strain curve are greatly influenced by the value of κ as shown in Fig. 8 (a), i.e. the smaller value of κ gives the smaller prediction of γ and the greater rate of decrease of p for a given stress ratio η.

Wroth and Bassett (1965) proposed a new predicting method of stress-strain relationship of soils based on the energy theory and exponential function. Parameters a and b in this theory, which was primarily concerned on sandy soil, have to be determined so as to make the predicted values best fitted to the experimental data. In application of this theory to normally consolidated clay, Wroth (1965) assumed the parameter b to be zero, which necessitated the parameter a to be a function of M, λ, κ and e_0. Therefore, determination of the parameter κ in Wroth's stress-strain equation still remains as a problem because the parameter a, which was originally an experimental constant, became to be dependent on the value of κ.

Ohta et al. (1975) developed a stress strain theory for anisotropically consolidated clay, extending their previous theory (e.g. Hata et al., 1969) for isotropically consolidated clay. In this theory they derived following equation by using the condition of critical state.

$$\mu=\frac{\lambda-\kappa}{(1+e_0)M}$$

The parameter μ was originally defined as dilatancy index, but now it has a different definition, being dependent on M, λ and κ.

Predicted values by the theories of Wroth and Ohta et al. will be exactly the same as in Fig. 8(a), provided that the same value of M, λ and κ are used.

Roscoe and Burland (1968) introduced a new energy equation to their original concept to make some modifications to their previous theory. Fig. 8 (b) illustrates the comparison of observed stress path and stress ratio-strain curve with calculated ones by modified theory. As it was in Fig. 8 (a), the influence of the magnitude of κ value on the prediction of the stress-strain relationships is obviously dominant.

Karube (1977) proposed a method to obtain incremental stress-strain relationship, based on an experimental relationship between strain increment ratio versus stress ratio. His equations contain an experimental parameter α which is determined so as to make the best fit to observed stress ratio-strain curve. Fig. 8(c) shows the comparison between observed and predicted stress paths and stress ratio versus strain curves. Stress ratio-strain curve for $\alpha=0.025$ gives the best fit, but the failure point in the predicted stress path is appreciably different from the observed one. Calculated stress paths for $\alpha=0.02$ and 0.03 are also illustrated in the same figure, and they indicate that a satisfying stress path prediction can not be obtained by merely modifying the value of α.

STRESS-STRAIN PREDICTION WITH DILATANCY FUNCTION $F(\eta)$

Introduction

In the preceding section, the authors examined the validity of the existing theories by comparing the observed with predicted stress-strain relationship. In Cam-Clay equation (and also Wroth's and Ohta's theory) three basic parameters M, λ and κ are needed to fix. Among these parameters, the appropriate value of κ is difficult to determine objectively, since it varies with overconsolidation ratio. Modified theory by Roscoe & Burland

and Karube's theory also have the same problem concerning the value of κ.

The authors derived a new stress-strain equation under the assumptions as shown in the following section. Special features of the equation are as follows

1) the equation involves the dilatancy function $F(\eta)$ which represent appropriately the dilatancy characteristics of soils, and

2) κ is not considered to be a material constant, but a parameter which is determined from the critical state condition. Since the value of κ thus determined is not a material constant, a new symbol ν in place of κ will be used in this paper to make clear the difference of their outcoming. Although the two parameters κ and ν are determined by different ways, their functions are exactly the same in the sense of Cam-Clay equations.

Assumptions

Referring to the existing theories and taking $F(\eta)$ and ν into consideration, the authors made following assumptions to derive a new stress-strain equations.

1) Total change of void ratio during shear is represented by summation of void ratio change due to isotropic stress component $(de)_c$ and that due to deviatoric one, $(de)_d$ (Eq. (1)).

2) The change of void ratio due to isotropic stress is represented by Eq. (2).

3) Void ratio change due to deviatoric stress is represented by Eq. (3).

4) Recoverable component of the change of void ratio is given as follows

$$(de)^r = -\nu dp/p \tag{6}$$

5) There is no recoverable component of shear strain during shear, and so

$$(d\gamma)^r = 0 \tag{7}$$

6) Normality rule can be conveniently used to obtain incremental stress-strain relationship.

$$\frac{1/3\,dv^p}{d\gamma^p} = -\frac{d\tau}{dp} \tag{8}$$

Incremental Stress-Strain Equations

Plastic Volumetric strain increment dv^p is given as follows

$$dv^p = dv - dv^r = -\frac{1}{1+e}(de + \nu\, dp/p) \tag{9}$$

From Eq. (1), (2), (3) and (9)

$$\begin{aligned} dv^p &= -\frac{1}{1+e}\left[-\lambda\frac{dp}{p} - (1+e_0)F'(\eta)d\eta + \nu\frac{dp}{p}\right] \\ &= \frac{1+e_0}{1+e}\left[\frac{\lambda-\nu}{1+e_0}\cdot\frac{dp}{p} + F'(\eta)d\eta\right] \end{aligned} \tag{10}$$

Integrating Eq. (6) with the condition $e=e_0$ and $p=p_0$, and combining the resulting equation with Eq. (4), following equation is obtained to represent the current yield locus.

$$\frac{\lambda-\nu}{1+e_0}\ln\frac{p}{p_0} + F(\eta) - F(\eta_0) = 0 \tag{11}$$

Accordingly successive yield loci is given by the equation.

$$\frac{\lambda-\nu}{1+e_0}\ln\frac{p}{p_{0i}} + F(\eta) - F(\eta_0) = 0 \tag{12}$$

, where p_{0i} is effective mean stress at the intersection point of consolidation and swelling lines.

Differentiation of Eq. (12) leads to

$$\frac{d\tau}{dp}=\frac{-\dfrac{\lambda-\nu}{1+e_0}}{F'(\eta)}+\eta \tag{13}$$

Substituting Eq. (13) into Eq. (8), relationship between plastic strain increment ratio versus stress ratio is obtained as follows

$$\frac{d\gamma^p}{dv^p}=-\frac{1}{3}\frac{dp}{d\tau}=-\frac{1}{3}\left[\frac{F'(\eta)}{\eta F'(\eta)-\dfrac{\lambda-\nu}{1+e_0}}\right] \tag{14}$$

, and substitution of Eq. (10) into the above equation gives

$$d\gamma^p=-\frac{1}{3}\frac{1+e_0}{1+e}\left[\frac{\lambda-\nu}{1+e_0}\frac{dp}{p}+F'(\eta)d\eta\right]\frac{F'(\eta)}{\eta F'(\eta)-\dfrac{\lambda-\nu}{1+e_0}} \tag{15}$$

Furthermore, from Eq. (1), (2) and (3)

$$dv=\frac{-de}{1+e_0}=\frac{\lambda}{1+e_0}\frac{dp}{p}+F'(\eta)d\eta \tag{16}$$

Since $dv=0$ in the undrained test,

$$\frac{\lambda}{1+e_0}\frac{dp}{p}+F'(\eta)d\eta=0 \tag{17}$$

Combining Eq. (17) with (15) and assuming $e=e_0$, following incremental stress ratio-strain equation for undrained test is obtained.

$$d\gamma=d\gamma^p=-\frac{\nu}{3\lambda}\cdot\frac{[F'(\eta)]^2}{\eta F'(\eta)-\dfrac{\lambda-\nu}{1+e_0}}d\eta \tag{18}$$

Roscoe et al. defined the critical state to be the state that shear strain continues to increase without further change of voids ratio or of the effective stresses. Considering the critical state to be that shear strain continues to increase without the change of stress ratio, following condition is satisfied at the critical state.

$$\left(\frac{d\eta}{d\gamma}\right)=0 \quad \text{at} \quad \eta=M \tag{19}$$

From Eq. (18) and (19), the parameter ν is determined as follows

$$\nu=\lambda-(1+e_0)MF'(M) \tag{20}$$

Thus the parameter ν can be obtained by the known parameters λ, e_0, M and $F'(M)$.

Determination of $F(\eta)$

The stress-strain equation mentioned above is based on the dilatancy function $F(\eta)$. Therefore, to describe accurately the stress-strain behaviour of a soil, it is necessary to find out the appropriate function of $F(\eta)$ to represent the stress-dilatancy characteristics of the soil.

As can be seen in Figs. 7 (a) and (b), it appears almost impossible to approximate the stress ratio-dilatancy plot by a single strainght line. Instead, it would be better to assume an appropriate curve or to approximate by a set of two straight lines. As a first approximation, the latter is assumed. According to this assumption, observed stress ratio-dilatancy relationships obtained from *NIC* and *NIE* tests are represented as follows (see Fig. 9). In *NIC* test,

$$F_1(\eta)=\mu_1\eta \quad \text{for} \quad 0\leqq\eta\leqq\eta_1 \tag{21 a}$$

and

$$F_2(\eta)=\mu_1\eta_1+\mu_2(\eta-\eta_1) \quad \text{for} \quad \eta_1<\eta\leqq M_c \tag{21 b}$$

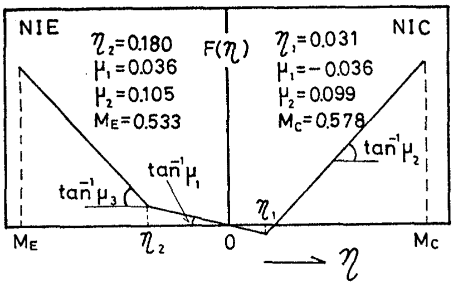

Fig. 9. Schematic diagram of stress ratio vs. dilatancy

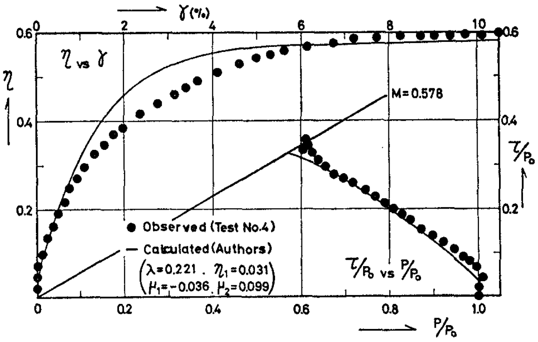

Fig. 10. Observed and predicted stress-strain relationship by the present theory

, and in *NIE* test,

$$F_1(\eta)=\mu_1\eta \quad \text{for} \quad 0\leqq\eta\leqq\eta_2 \tag{22 a}$$

and

$$F_2(\eta)=\mu_1\eta_2+\mu_3(\eta-\eta_2) \quad \text{for} \quad \eta_2<\eta\leqq M_E \tag{22 b}$$

, where η_1 and η_2 are the stress ratios at which dilatancy coefficient changes its value in compression and extension test respectively, and μ_1, μ_2 and μ_3 are the dilatancy coefficients as shown in Fig. 9, and M_C and M_E are equal to η at the critical state in compression and extension tests, respectively.

Stress path for *NIC* test is obtained by inserting Eqs. (21 a) and (21 b) into Eq. (5) as follows

$$p/p_0=\exp\left[-\frac{(1+e_0)\mu_1}{\lambda}\eta\right] \quad \text{for} \quad 0\leqq\eta\leqq\eta_1 \tag{23 a}$$

$$p/p_0=\exp\left[-\frac{1+e_0}{\lambda}\{\mu_1\eta_1+\mu_2(\eta-\eta_1)\}\right] \quad \text{for} \quad \eta_1<\eta\leqq M_C \tag{23 b}$$

Combining Eqs. (21 a) & (21 b) with Eq. (18) and integrating the resulting equations with initial condition $\gamma=0$ at $\eta=0$, equations for stress ratio-strain prediction can be derived as follows

$$\gamma=\frac{\nu\mu_1}{3\lambda}\left[\ln\left|\frac{\dfrac{\lambda-\nu}{1+e_0}}{\mu_1\eta-\dfrac{\lambda-\nu}{1+e_0}}\right|\right] \quad \text{for} \quad 0\leqq\eta\leqq\eta_1 \tag{24 a}$$

and

$$\gamma=\frac{\nu}{3\lambda}\left[\mu_1\ln\left|\frac{\dfrac{\lambda-\nu}{1+e_0}}{\mu_1\eta_1-\dfrac{\lambda-\nu}{1+e_0}}\right|+\mu_2\ln\left|\frac{\mu_2\eta_1-\dfrac{\lambda-\nu}{1+e_0}}{\mu_2\eta-\dfrac{\lambda-\nu}{1+e_0}}\right|\right] \quad \text{for} \quad \eta_1<\eta\leqq M_C \tag{24 b}$$

For *NIE* test, similar equations as shown above can be obtained.

Comparisons of Predicted with Observed Stress-Strain Relationship

In this section, the validity of the present method for estimating the undrained stress-strain behaviour of isotropically consolidated clay is examined. The data used for this purpose are those from *NIC*-No. 4, which was also used in preceding section. Parameters prepared for prediction are as follows

$$M=0.578 \qquad \lambda=0.221 \qquad e_0=1.339$$

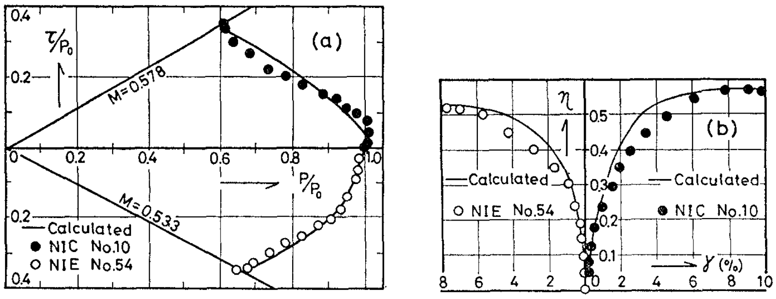

Fig. 11. Observed and predicted stress-strain relationship for both compression and extension tests by the present theory

$$\mu_1=-0.036 \qquad \mu_2=0.099 \qquad \eta_1=0.031$$

where the parameters except for e_0 are average values obtained from the series of *NIC* test.

Fig. 10 shows the comparison of the calculated stress paths and stress ratio–strain relationship with the observed ones. Fig. 11 (a) & (b) illustrate another example of comparisons including that of *NIE* test. As seen from these figures, both calculated stress paths and stress ratio–strain curves agree fairly well with the observed ones. It is a matter of course that the calculated stress path agrees with the observed one, because the predicted stress path was based on the measured $F(\eta)$ versus η relationship. However, the fact that the calculated stress ratio–strain curve agrees well with the observed one suggests that the normality rule may be conveniently used as far as the stress ratio–dilatancy characteristics could be closely approximated by appropriate function, in spite of some criticism on the validity of normality rule in soils.

PREDICTION OF STRESS-STRAIN BEHAVIOUR OF K_0 CONSOLIDATED CLAY

Introduction

The ultimate object of this paper is to find out a method by which the stress–strain behaviour of K_0 consolidated clay can be predicted, using the data obtained from isotropically consolidated undrained tests. Existing theories on this problem are as follows.

Ohta et al. (1975) assumed that the soil constants λ, κ and μ remain essentially unchanged, and the only difference between K_0 and isotropically consolidated specimens is the stress anisotropy. They proposed a method to predict stress–strain behaviour of K_0 consolidated clay, in which the stress path of K_0 consolidated clay is assumed to be obtained by shifting that of isotropically consolidated clay parallel to the ordinate and moving the starting point up to the point (p_0, τ_0), where p_0 and τ_0 are the octahedral normal and shear stresses at the end of K_0 consolidation. The method of Roscoe & Burland (1968) is essentially the same as Ohta et al.

Lewin (1975) suggested a method to obtain the undrained stress path for anisotropically consolidated clay using that of isotropically consolidated clay. Proposed method is as follows. Rendulic stress path for isotropically consolidated undrained test is regarded as being symmetrical about the space diagonal. For a specimen consolidated anisotropically along the anisotropic consolidation line at an angle α to space diagonal, the new axis of symmetry is drawn at an angle θ from the 'hinge-point' taken to be halfway along the space diagonal. Then, stress path for anisotropically consolidated specimen is produced by rotating that for isotropically consolidated specimen by the angle θ about the hinge-point, where the relationship between α and θ for a soil must in advance be determined experimentally.

Assumptions for Predicting the Stress-Strain Behaviour of K_0 Consolidated Clay

Referring to the methods mentioned above, the authors made following hypotheses to establish the predicting method of stress-strain relationship for K_0 consolidated clay.

1) Stress path for K_0 consolidated compression test

Stress path for NK_0C test in $p/p_0-\tau/p_0$ co-ordinate (see Fig. 12) is similar to that obtained by rotating the *NIC* stress path by an angle θ_0 after shifting the *NIC* stress path from the point (1, 0) to $(1, \tau_0/p_0)$, where

$$\theta_0=\tan^{-1}\tau_0/p_0$$

and, p_0 and τ_0 are the octahedral normal and shear stresses after K_0 consolidation.

2) Stress path for K_0 consolidated extension test

Stress path is similar to that obtained by rotating the *NIE* stress path by an angle $\theta_0/2$, after shifting the *NIE* stress path from the point (1, 0) to $(1, \tau_0/p_0)$. In addition, the effective mean stress at failure is equal to that of isotropically consolidated specimen.

Two hypotheses mentioned above are based on the following consideration that the stress-strain-strength properties of initially K_0 consolidated clay are clearly different from those of isotropically consolidated clay due not only to induced anisotropic stress system but also to structural anisotropy developed during consolidation. The authors assumed that the stress anisotropy is covered by shifting the starting point of shear from $\tau=0$ plane to $\tau=\tau_0$ plane. Although quantitative evaluation of structural anisotropy is a difficult problem to solve, it may roughly be done as follows. Structural difference between test specimens after K_0 and isotropic consolidation appears markedly in compression test, because the direction of major principal stress during shear is the same as that in consolidation. Therefore, the structural difference for this case is assumed as being expressed by the magnitude of rotating angle θ_0. On the other hand, structural difference between *NIE* and NK_0E almost disappears during initial part of shear, during which interchange in principal stress directions occurs, and the stress-strain behaviour during later part of shear is almost the same in two test, especially at critical state. These considerations lead to the assumption that the difference may roughly be expressed by the angle $\theta_0/2$ and the effective mean stress at failure in NK_0E test is almost equal to that in *NIE* test.

Predicted Stress-Strain Behaviour

Based on the preceding hypotheses, prediction of NK_0C and NK_0E stress-strain relationship using *NIC* and *NIE* test data will be made.

1) Prediction of stress-strain behaviour from *NIC* test data

As shown in preceding section, stress ratio-dilatancy characteristics in *NIC* is expressed approximately by Eq. (21). Shifting these relations from $F(\eta)=0$ at $\eta=0$ to $F(\eta)=0$ at $\eta=\eta_0$, following equations are obtained.

$$F_1(\eta)=\mu_1(\eta-\eta_0) \quad \text{for} \quad 0<\eta-\eta_0\leqq\eta_1 \tag{25 a}$$

$$F_2(\eta)=\mu_1\eta_1+\mu_2(\eta-\eta_0-\eta_1) \quad \text{for} \quad \eta-\eta_0>\eta_1 \tag{25 b}$$

Octahedral effective normal and shear stresses normalized by the initial octahedral normal stress p_0 at any value of $\eta(\eta>\eta_0)$ after shifting the *NIC* stress path are represented, referring to Eq. (5), as follows

$$p/p_0=\exp\left[-\frac{1+e_0}{\lambda}F(\eta)\right] \tag{26 a}$$

$$\tau/p_0=\eta\cdot p/p_0 \tag{26 b}$$

Next step is to rotate the stress path by an angle θ_0 around the point $(1, \tau_0/p_0)$. Then,

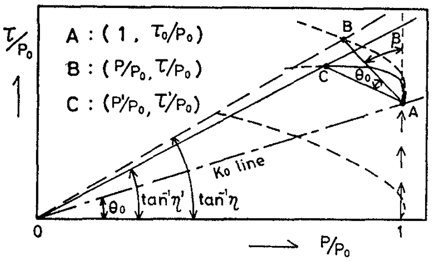

Fig. 12. Stress path prediction for NK_0C test

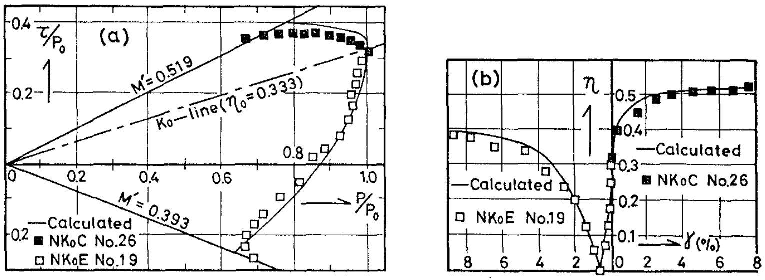

Fig. 13. Observed and predicted stress-strain relationship for K_0 consolidiated clay

the co-ordinates of stress point after rotation are represented, referring to Fig. 12, as follows

$$\tau'/p_0=\eta_0+\sqrt{(\tau/p_0-\eta_0)^2+(1-p/p_0)^2}\cos(\beta+\theta_0) \tag{27 a}$$

$$p'/p_0=1-\sqrt{(\tau/p_0-\eta_0)^2+(1-p/p_0)^2}\sin(\beta+\theta_0) \tag{27 b}$$

, where

$$\beta=\tan^{-1}\frac{p_0-p}{\tau-\tau_0}$$

Combination of Eqs. (5) with (27 b) gives a new $F(\eta)$ versus η relationship, and new dilatancy equations equivalent to Eqs. (21 a) & (21 b) can also be obtained as follows

$$F_1(\eta)=\mu_1'(\eta-\eta_0) \quad \text{for} \quad 0<\eta-\eta_0\leqq\eta_1' \tag{28 a}$$

$$F_2(\eta)=\mu_1'(\eta_1'-\eta_0)+\mu_2'(\eta-\eta_1') \quad \text{for} \quad \eta_1'<\eta \tag{28 b}$$

Parameters η_1', μ_1' and μ_2' are equivalent to η_1, μ_1 and μ_2 in Eqs. (25 a) & (25 b), respectively. A new strength parameter M' is obtained by putting $\eta=M$ into Eqs. (26) and (27). Furthermore, replacing the value M and $F'(M)$ in Eq. (20) by M' and $F'(M')$, following equation is obtained.

$$\nu'=\lambda-(1+e_0)M'F'(M') \tag{29}$$

Combination of Eqs. (28) & (29) with Eq. (18) and integration of the resulting equations with initial condition $\gamma=0$ at $\eta=\eta_0$, following stress ratio-strain equations for K_0 consolidated clay can be obtained.

$$\gamma=\frac{\nu'\mu_1'}{3\lambda}\ln\left|\frac{\mu_1'\eta_0-\dfrac{\lambda-\nu'}{1+e_0}}{\mu_1'\eta-\dfrac{\lambda-\nu'}{1+e_0}}\right| \quad \text{for} \quad 0<\eta-\eta_0\leqq\eta_1' \tag{30 a}$$

$$\gamma=\frac{\nu'}{3\lambda}\left[\mu_1'\ln\left|\frac{\mu_1'\eta_0-\dfrac{\lambda-\nu'}{1+e_0}}{\mu_1'\eta_1'-\dfrac{\lambda-\nu'}{1+e_0}}\right|+\mu_2'\ln\left|\frac{\mu_2'\eta_1'-\dfrac{\lambda-\nu'}{1+e_0}}{\mu_2'\eta-\dfrac{\lambda-\nu'}{1+e_0}}\right|\right] \quad \text{for} \quad \eta_1'<\eta \tag{30 b}$$

2) Prediction of NK_0E stress-strain behaviour from NIE test data

Stress-strain prediction of NK_0E test using NIE test data can be performed by almost the same procedure as in compression test, except that the angle of rotation is $\theta_0/2$ and the effective mean stress at failure is set to be equal in NIE and NK_0E test.

The comparison of the stress paths and stress ratio-strain curves for NK_0C & NK_0E tests predicted by the present method with those observed indicates fairly good agreement as shown in Fig. 13 (a) & (b). By the way, the values of strength parameter M' for NK_0C and NK_0E in Fig. 13 (a) are the predicted ones, while the corresponding observed average values are given previously in Fig. 4. Comparison of these values with each other indicates a good agreement.

Therefore, estimation is now possible on the undrained compression and extension stress–strain–strength behaviour of K_0 consolidated clay using the data obtained from isotropically consolidated undrained compression and extention tests. Parameters for estimation are the coefficient of earth pressure at rest K_0, strength parameter M, compression index λ and dilatancy function $F(\eta)$.

CONCLUSIONS

1) The difference of stress system (or the difference of relative magnitude of intermediate stress) during shear affects the stress ratio–strain relationship, but the type of stress application, i.e. increasing or decreasing stress, in extension tests does not make any influence upon the stress ratio–strain properties of clay.

2) Effective angle of shearing resistance ϕ' in undrained compression and extension tests are affected by the stress anisotropy during consolidation.

3) The ratio of undrained shear strength to effective vertical consolidation pressure is greatly influenced by the difference of stress system, especially in K_0 consolidated clay, and it seems that the higher the plasticity of clay, the smaller the influences of stress system during shear.

4) Octahedral effective stress ratio–dilatancy curves obtained from undrained compression and extension tests can be approximated by a set of two strainght lines.

5) Isotropically consolidated undrained compression and extension stress–strain behaviour of clay is described by using dilatancy function $F(\eta)$ and normality rule in conjunction with the basic soil constants M and λ.

6) Stress–strain–strength behaviour of K_0 consolidated clay during undrained compression and extension tests can be predicted by using the data obtained from isotropically consolidated undrained compression and extension tests.

ACKNOWLEDGEMENT

The authors wish to thank Messrs. S. Takeda and S. Kondo who contributed to this study in developing the loading extension test apparatus and in making calculations. They are also indebted to Messrs. K. Ichikubo, O. Sawamukai, Y. Kamei and H. Sato who conducted major part of the experiment, and to Mr. Y. Kudo for his preparation of the figures. The present study was undertaken by the financial aid of a research grant from the Ministry of Education.

NOTATION

K_0 = coefficient of earth pressure at rest
NIC = isotropically consolidated undrained compression test
NIE = isotropically consolidated undrained extension test
$NIEL$ = isotropically consolidated undrained loading extension test
NK_0C = K_0 consolidated undrained compression test
NK_0E = K_0 consolidated undrained extension test
NK_0EL = K_0 consolidated undrained loading extension test
a, b = experimental parameters in stress–strain equation by Wroth and Bassett
e_0 = void ratio of clay after consolidation
p = octahedral effective normal stress $p=(\sigma_1'+\sigma_2'+\sigma_3')/3$
p_0 = octahedral effective normal stress after consolidation
p_v = effective vertical stress after consolidation
p_{0i} = effective mean stress at the intersection point of consolidation and swelling lines
s_u = undrained shear strength

v = volumetric strain
v^r, v^p = recoverable and irrecoverable components of v
x, x_0 = stress ratios normalized by M, $x=\eta/M$, $x_0=\eta_0/M$
M = octahedral stress ratio at critical state
M_C, M_E = M in compression and extension tests
α = experimental parameter in stress-strain equation by Karube
β = angle representing the location of stress point (Fig. 12)
γ = octahedral shear strain $\gamma=1/3\sqrt{(\varepsilon_1-\varepsilon_2)^2+(\varepsilon_2-\varepsilon_3)^2+(\varepsilon_3-\varepsilon_1)^2}$
γ^r, γ^p = recoverable and irrecoverable components of γ
η = octahedral stress ratio $\eta=\tau/p$
η_0 = octahedral stress ratio after anisotropic consolidation
η_1, η_2 = η at the inflection point in $F(\eta)$ vs. η curve (Fig. 9)
θ_0 = angle representing the magnitude of stress anisotropy (Fig. 12)
κ = inclination of swelling line in $e-\ln p$ diagram
λ = inclination of normal consolidation line in $e-\ln p$ diagram
μ = dilatancy coefficient
μ_1, μ_2, μ_3 = dilatancy coefficients (Fig. 9)
ν = coefficient correspond to κ (Eq. 20)
$\sigma_1', \sigma_2', \sigma_3'$ = major, intermediate and minor effective principal stresses
τ = octahedral shear stress $\tau=1/3\sqrt{(\sigma_1-\sigma_2)^2+(\sigma_2-\sigma_3)^2+(\sigma_3-\sigma_1)^2}$
τ_0 = octahedral shear stress after anisotropic consolidation
ϕ' = effective angle of shearing resistance
ϕ_C', ϕ_E' = ϕ' in compression and extension tests
$F(\eta)$ = dilatancy function

REFERENCES

1) Akai, K. and Adachi, T. (1965): "Study on the one-dimensional consolidation and the shear strength characteristics of fully-saturated clay, in terms of effective stress," Trans., JSCE, No. 113, pp. 11-27 (in Japanese).
2) Broms, B. B. and Casbarian, A. O. (1965): "Effects of rotation of principal stress axes and of the intermediate principal stress on the shear strength," Proc., 6th ICSMFE, Vol. 1, pp. 179-183.
3) Hata, S., Ohta, H. and Yoshitani, S. (1969): "On the state surface of soils," Proc., JSCE, No. 172, pp. 71-92.
4) Henkel, D. J. (1960): "The shear strength of saturated remolded clays," Proc., ASCE Research Conf. on Shear Strength of Cohesive Soils, Boulder, Colorado, pp. 533-554.
5) Henkel, D. J. and Sowa, V. A. (1963): "The influence of stress history on stress paths in undrained triaxial tests on clay," Laboratory Shear Testing of Soils, ASTM, STP, No. 361, pp. 280-291.
6) Karube, D. (1975): "Special testing methods other than standardized triaxial test and their problems," Proc., 20th Symposium on Soil Mechanics, JSSMFE, pp. 45-60 (in Japanese).
7) Karube, D. (1977): "A stress-strain-time equation of normally consolidated clay," Proc., 9th ICSMFE, Specialty Session No. 9, pp. 105-112.
8) Kitago, S., Mitachi, T. and Kamiya, M. (1976): "Strength properties of saturated clay in undrained triaxial extension," Proc., 11th Annual Meeting of JSSMFE, pp. 239-242 (in Japanese).
9) Kitago, S. et al. (1978): "Undrained shear strength characteristics of clay-glass beads mixtures," Technical Report, JSSMFE, Hokkaido Branch, No. 18, pp. 167-176 (in Japanese).
10) Ladd, C. C. (1965): "Stress-strain behaviour of anisotropically consolidated clays during undrained shear," Proc., 6th ICSMFE, Vol. 1, pp. 282-286.
11) Ladd, C. C. (1973): Discussion, Main Session IV, Proc., 8th ICSMFE, Vol. 4-2, pp. 108-115.
12) Lade, P. V. (1976); "Three-dimensional behaviour of normally consolidated cohesive soil,"

Report to the National Science Foundation.
13) Leon, J. L. and Alberro, J. (1977): "Extension and compression tests on Mexico City clay," Proc., 9th ICSMFE, Vol. 1, pp. 193-196.
14) Lewin, P. I. (1975): "Plastic deformation of clay with induced anisotropy," Istanbul Conf. on SMFE, Vol. 2, pp. 137-148.
15) Mikasa, M., Nishigaki, Y. and Okajima, Y. (1978): "Comparison of the ratio c_u/p obtained from different types of test," Proc., 13th Annual Meeting of JSSMFE, pp. 325-328 (in Japanese).
16) Mitachi, T. and Kitago, S. (1976): "Change in undrained shear strength characteristics of saturated remolded clay due to swelling," Soils and Foundations, Vol. 16, No. 1, pp. 45-58.
17) Ohta, H., Yoshitani, S. and Hata, S. (1975): "Anisotropic stress-strain relationship of clay and its application to finite element analysis," Soils and Foundations, Vol. 15, No. 4, pp. 61-79.
18) Parry, R. H. G. (1960): "Triaxial compression and extension tests on remoulded saturated clay," Geotechnique, Vol. 10, No. 4, pp. 166-180.
19) Parry, R. H. G. and Nadarajah, V. (1973): "Observations on laboratory prepared, lightly overconsolidated specimens of kaolin," Geotechnique, Vol. 24, No. 3, pp. 345-358.
20) Roscoe, K. H. and Burland, J. B. (1968): "On the generalized stress-strain behaviour of wet clay," Engineering Plasticity, Cambridge Univ. Press, pp. 535-609.
21) Roscoe, K. H., Schofield, A. N. and Thurairajah, A. (1963): "Yielding of clays in states wetter than critical," Geotechnique, Vol. 13, No. 3, pp. 211-240.
22) Sawada, T., Hasegawa, T. and Shimada, K. (1977): "On the volume change characteristics of normally consolidated clays," Proc., 12th Annual Meeting of JSSMFE, pp. 315-318 (in Japanese).
23) Scott, R. F. (1963): Principles of Soil Mechanics, Addison-Wesley Publishing Co., Reading, Mass.
24) Shibata, T. and Karube, D. (1965): "Influence of the variation of the intermediate principal stress on the mechanical properties of normally consolidated clay," Proc., 6th ICSMFE, Vol. 1, pp. 359-363.
25) Shibata, T., Ohta, H. and Sekiguchi, H. (1976): "Stress-strain-strength characteristics of soil," Tsuchi-to-Kiso, JSSMFE, Vol. 24, No. 8, pp. 11-22 (in Japanese).
26) Tsushima, M. and Miyakawa, I. (1977): "Experimental consideration on the strength properties of undisturbed organic soils," Proc., Symposium on the Engineering Properties of Organic Soils, JSSMFE, pp. 53-56 (in Japanese).
27) Vaid, Y. P. and Campanella, R. G. (1974): "Triaxial and plane strain behaviour of natural clay," Proc., ASCE, Vol. 100, GT 3, pp. 207-224.
28) Wroth, C. P. (1965): "The prediction of shear strains in triaxial tests on normally consolidated clays," Proc., 6th ICSMFE, Vol. 1, pp. 417-420.
29) Wroth, C. P. and Bassett, R. H. (1965): "A stress-strain relationship for the shearing behaviour of a sand," Geotechnique, Vol. 15, No. 2, pp. 32-56.
30) Wu, T. H., Loh, A. K. and Malvern, L. E. (1963): "Study of failure envelopes of soils," Proc., ASCE, Vol. 89, SM 1, pp. 145-181.

(Received August 26, 1978)